Chemical Engineering Journal 155 (2009) 260–265

Contents lists available at ScienceDirect

Chemical Engineering Journal

journal homepage: www.elsevier.com/locate/cej

Study of SCR cold-start by energy method

Yong Miao [a], Lea-Der Chen [b,*], Yongsheng He [a], Tang-wei Kuo [a]

[a] General Motors Company, 30500 Mound Rd, Warren, MI 48090, USA
[b] Department of Mechanical and Industrial Engineering, The University of Iowa, 2416B Seamans Center, Iowa City, IA 52242, USA

ARTICLE INFO

Article history:
Received 21 March 2009
Received in revised form 9 July 2009
Accepted 30 July 2009

Keywords:
Catalyst light-off
Energy balance
Exhaust aftertreatment
NOx selective catalytic reduction

ABSTRACT

The cold-start of a prototype diesel engine exhaust aftertreatment system was analyzed using a simplified energy balance to study the impact of system design changes on the performance of the selective catalytic NOx reduction reactor. The simplified energy balance method is shown to be a viable tool for system-level analysis of the aftertreatment performance. The results indicate that without an external energy supply the best way to shorten the selective catalytic reduction (SCR) reactor light-off time is to reduce the system thermal inertia by including a metallic diesel oxidation catalyst (DOC) and moving the SCR reactor upstream. Such optimization of the aftertreatment architecture is found to significantly reduce SCR light-off time for the configurations examined. Electrical heating applied to the SCR and DOC reactors can also reduce the light-off time. The system architecture optimization, however, is subject to vehicle under-hood packaging restrictions. To meet more stringent emission standards in the future, a combination of architecture optimization and electrical heating will be required.

1. Introduction

Diesel (compression-ignition) engines can be run at higher compression ratios, which result in higher thermal efficiencies compared to gasoline (spark-ignition) engines [1]. As a consequence, diesel engines can reduce green house gas emissions based on the same mileage driven in comparison to gasoline engines. One challenge for the diesel engine is the removal of NOx (nitrogen oxides) from the exhaust, which is a major source of acid rain and chemical smog [2]. It can also cause respiratory problems for people [3]. The selective catalytic reduction (SCR) of NOx is a promising technology for NOx reduction [4]. However, challenges remain during the cold-start of diesel engines.

The cold-start emission contributes greatly to the overall automobile tailpipe emission [5]. During the cold-start, most of the target emission species (CO, hydrocarbons, and NOx) pass through the catalytic converter with no apparent conversion due to the low reactivity at low temperatures. For larger diesel engines, the problem is even worse because typical SCR reactors are about twice of the engine displacement volume and it requires a longer time to reach SCR light-off condition. Several factors such as urea dosing rate, urea decomposition and mixing, NO to NO_2 ratio can affect SCR performance after light-off. However, significant NOx slip before SCR light-off is the main barrier to meeting T2B5 (Tier 2 Bin 5) emission standards [6]. Conversely, T2B5 emission standards cannot be met even with state-of-the-art catalysts and 100% NOx conversion after SCR light-off. Reducing the aftertreatment system warm-up time to reduce the emission during the cold-start period is necessary to meet T2B5 emission standards.

The CFD-based model is widely used to predict the aftertreatment device performance [7,8] as well as the whole aftertreatment system [9]. This approach gives potentially accurate results; however, it requires detail knowledge about the kinetics of catalytic reactions, which is generally lacking. Compared to the one-dimensional (1D) CFD model, the energy balance analysis has several advantages. It does not require reaction kinetics nor does it require robust solvers for the stiff differential equations [10]. The energy balance method can provide instant thermal characteristics of the aftertreatment system with acceptable accuracy. Savings in product development time and cost can be realized.

In this paper, an example aftertreatment system of a 4.5 l diesel engine is used to demonstrate how the energy balance method can be applied for the cold-start analysis. The architecture of the aftertreatment system is shown in Fig. 1. The first diesel oxidation catalyst (DOC) is placed closest to the engine to facilitate quick light-off. The reaction heat from carbon monoxide (CO) and hydrocarbons (HC) oxidation can help to heat-up the downstream devices. Downstream the first DOC, there is a long pipe connected to SCR reactor for NOx reduction. The pipe consists of two sections connected by the urea injector body. The first section (closer to DOC) is about 1 m (or 39 in.) long, which is chosen in compliance with under-hood packaging restrictions. The second section, i.e., that between the urea injector body and SCR, is about 0.4 m (or 16 in.) long, which is intended for urea mixing. After SCR,

* Corresponding author. Tel.: +1 319 335 5674.
E-mail address: ldchen@engineering.uiowa.edu (L.-D. Chen).

1385-8947/$ – see front matter © 2009 Elsevier B.V. All rights reserved.
doi:10.1016/j.cej.2009.07.054

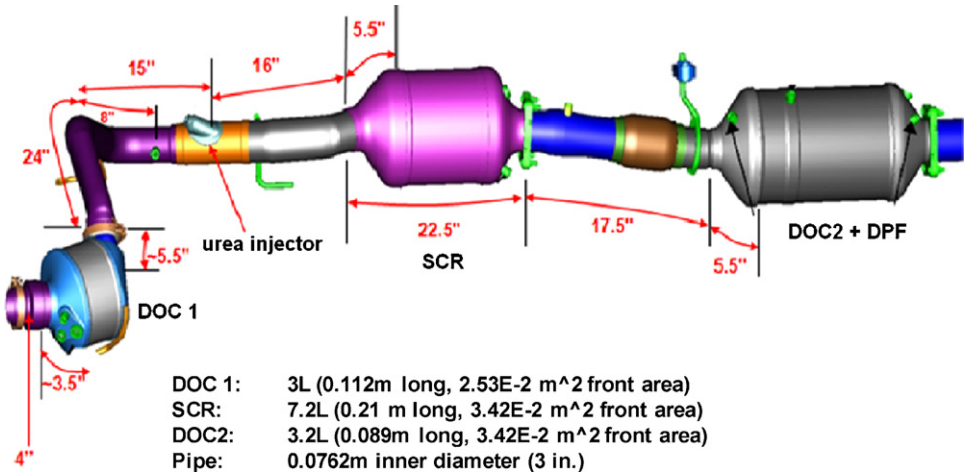

Fig. 1. Illustration of architecture of a prototype aftertreatment system for 4.5 l diesel engine.

there is a second DOC and a DPF (diesel particle filter) for soot removal.

The experimentally measured temperatures at SCR inlet and outlet, as well as the accumulated engine-out NOx emissions during a typical Federal Test Procedure-75 (FTP-75) driving cycle are plotted in Fig. 2. In the first 210 s, the SCR temperature is below the NOx reduction light-off temperature 473 K; no NOx reduction can be achieved during this period. For the NOx emission standard of T2B5 at the tail pipe (0.7×10^{-3} kg mile^{-1} for the FTP-75 test with driving distance of 11 miles), no matter how effective the SCR can be to reduce NOx after light-off, the FTP75 test fails due to the large amount of NOx emission during the SCR heat-up period. To meet this challenge, several methods to reduce the SCR light-off time are examined: moving SCR upstream (moving SCR closer to engine to reduce the pipe length between SCR and DOC), metallic DOC (to reduce thermal mass compared to ceramic DOC), and external electrical heating. The effectiveness of these methods is analyzed with the energy balance method.

2. Methodology

In brief, the cold-start is modeled a heat transfer process. That is to assume energy transfer from the hot exhaust gas to the cold aftertreatment devices (DOC, pipes, and SCR) and heat release from CO and HC oxidation in DOC to be the limiting mechanisms of the SCR light-off process. Based on the lumped capacitance formulation of heat transfer [11], the energy balance can be written for aftertreatment devices as follows:

$$(mC)_s \frac{\partial T_s}{\partial t} = (\dot{m}C)_g (T_g^{in} - T_g^{out}) + Q_{source} - Q_{loss} \quad (1)$$

where subscripts s and g stand for the solid and gas phases, respectively; superscripts *in* and *out* represent the inlet and outlet conditions, respectively; m is for the total mass of the element, C the specific heat, and $\dot{m}$ the mass flow rate. The left hand side of Eq. (1) is the energy accumulation inside the solid phase. The first term on the right hand side is the heat transfer between the exhaust gas and the solid phase (positive for heat transfer into the solid phase, and vice versa). The second term on the right hand side, Q_{source}, is the energy source term, including the reaction heat release from CO and HC oxidation (DOC only), and/or external heating by electricity. The third term, Q_{sink}, is the heat loss to the surroundings (pipe only).

It is assumed that thermal equilibrium is reached in each component/element of the aftertreatment system. Specifically, each element (DOC, pipe, and SCR) is assumed to have the same uniform temperatures for the solid and gas phases. As the result, a single energy balance equation is used. The thermal equilibrium assumption results in a significant saving in the computational cost when compared to the 1D or multi-dimensional CFD models. The energy balance, Eq. (1), is applied to each element along the gas flow direction.

The efficiency (reactivity) of DOC is a function of temperature. The catalytic reaction kinetic is complex [12]. To simplify the analysis, the DOC efficiency is assumed to follow the piecewise linear relationships with respect to DOC outlet temperature for fresh and aged DOC as shown in Fig. 3. The aged DOC is shown to have a higher light-off temperature than that of the fresh DOC. The light-off temperature shown in Fig. 3 is lower than that reported in literature because the calculated outlet temperature, instead of the inlet temperature, is used in this study. The reaction heat release term in Eq. (1) is calculated by Eq. (2):

$$Q_{rxn} = \sum_{k=1}^{n} \dot{m} Y_k^{inlet} f(T) \Delta h_k \quad (2)$$

where $f(T)$ is the linear function shown in Fig. 3, Δh_k the reaction enthalpy, and Y_k^{inlet} the mole fraction of reactant species (e.g., CO, HCs) at DOC inlet.

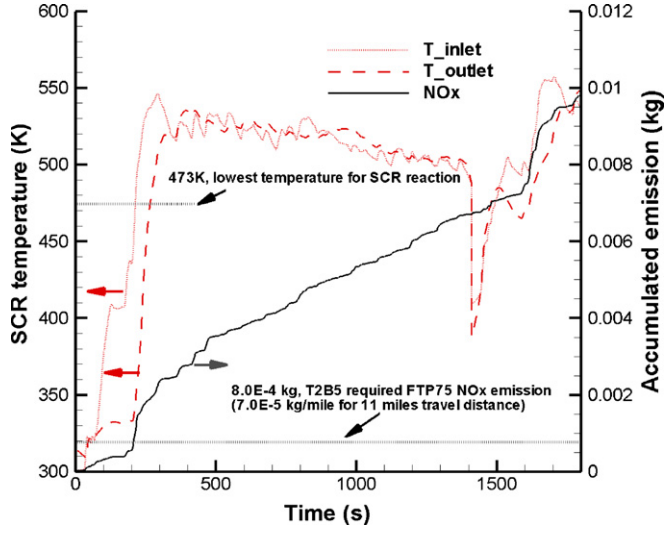

Fig. 2. Experimental results of temperature and accumulated NOx emission during FTP-75 test.

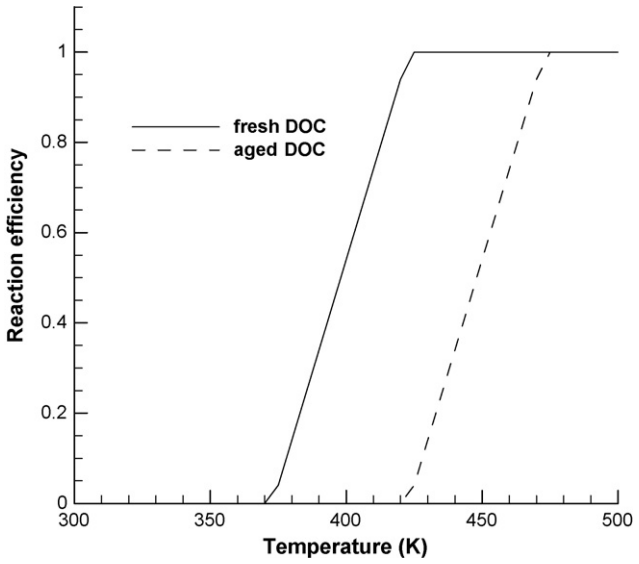

Fig. 3. Reaction efficiencies of fresh and aged DOC as functions of DOC outlet temperature.

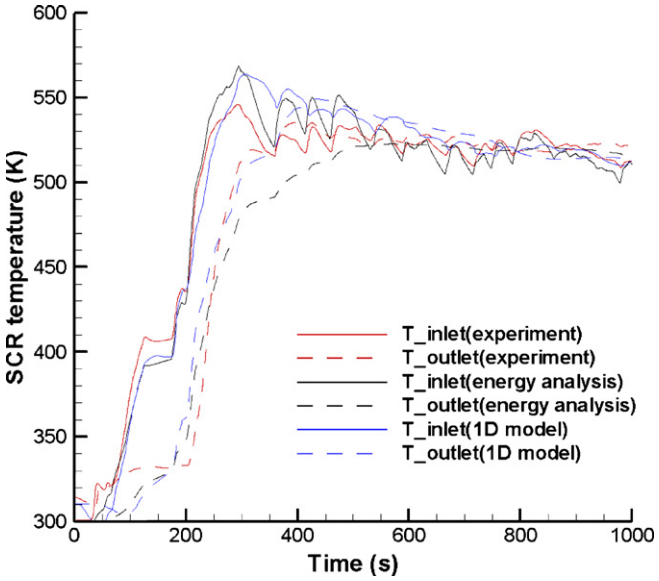

Fig. 5. Validation of temperature results at SCR inlet and outlet; aged DOC.

It is further assumed that heat loss only occurs in the pipe. The heat transfer rate to the surroundings due to convective and radiative heat transfer is obtained from:

$$Q_{\sin k} = hA(T_s - T_\infty) + \varepsilon\sigma A(T_s^4 - T_\infty^4) \quad (3)$$

where A is the heat transfer area which is proportional to the pipe length, h the convective heat transfer coefficient ($10\,W\,m^2\,K^{-1}$ is used in the study), T_∞ is the surrounding temperature (300 K is used), ε the emissivity of the pipe outer wall (0.8 is used), and σ the Boltzmann constant.

The mathematical model is validated by two sets of experimental data taken from the prototype aftertreatment system shown in Fig. 1. One fresh and one aged DOC, and two different engine-out conditions are examined. The same parameter values are used except for the respective DOC efficiencies.

Comparison between the model prediction and the experimental data is shown in Figs. 4 and 5. In general, the energy balance analysis captures the trends of thermal behavior (temperature) of the aftertreatment system with noted discrepancies due to simplifying assumptions. For example, error in the prediction of the SCR inlet temperatures between 75 and 175 s is attributed to the error associated with the prescribed DOC efficiencies. Error in the calculated SCR outlet temperatures below 373 K, or before 200 s, is due to neglect of the heat release from water condensation and ammonium nitrite formation. The simulation is seen to over-estimate the SCR inlet temperature, as well as SCR outlet temperature after light-off; this discrepancy is due to the fact that heat losses from DOC and SCR are not considered and that thermal equilibrium is not fully established in the components.

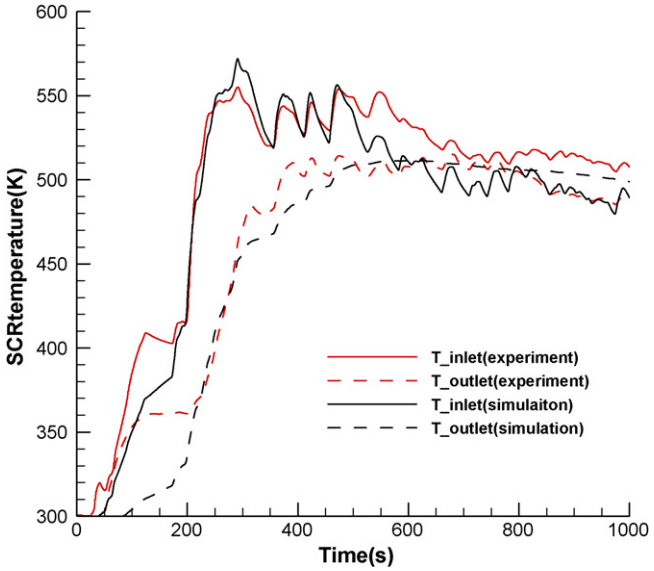

Fig. 4. Validation of temperature results at SCR inlet and outlet; fresh DOC.

The results of 1D simulation [13] of the aged DOC case are also plotted in Fig. 5. In the 1D model, transport equations of momentum, species and energy in conjunction with global reaction kinetics for DOC [12] and detailed surface reaction kinetics for SCR [14] are solved. This 1D model has been used in another study and shows its ability to capture the real engine aftertreatment system behavior [15]. Similar to the energy analysis method, error in the calculated SCR outlet temperatures before 200 s is due to neglect of the heat release from water condensation and ammonium nitrite formation. Before SCR light-off, the temperature predicted by energy balance model agrees well with the 1D simulation. Discrepancies as large as 45 K are seen after the light-off, or from 300 to 500 s, which suggests that thermal equilibrium assumption is no longer justifiable for the post-light-off condition. The 1D calculation lends support to thermal equilibrium assumption adopted for analysis of the cold-start period, i.e., from 0 to 250 s.

3. SCR cold-start analysis

NOx emission during the cold-start poses the greatest challenge to meet the more stringent regulation requirement. As shown in Fig. 2, it takes about 200 s for the SCR to reach the light-off temperature. A significant amount of NOx emission occurs during the SCR heat-up period. To meet the emission standard, the SCR light-off time must be reduced.

To study NOx emission during the cold-start, a simplified engine-out exhaust schedule is used. Instead of unsteady flow (i.e., time-dependent profiles of velocity, species concentrations and temperature) of actual engine-out conditions, a constant exhaust mass flow rate of $0.05\,kg\,s^{-1}$ is used. The CO oxidation is assumed to be the only exothermic reaction in the aftertreatment system

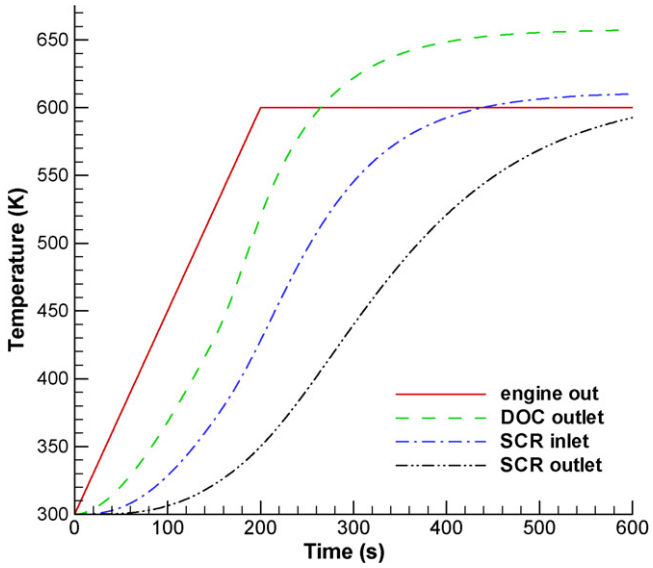

Fig. 6. Temperature at DOC outlet, SCR inlet and SCR outlet as functions of time, along with engine-out temperature.

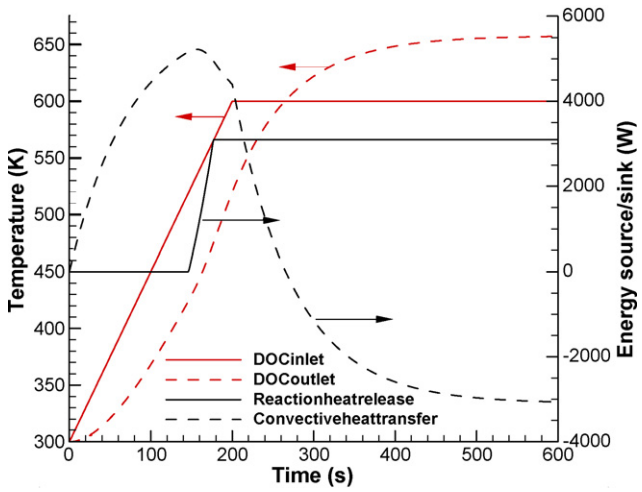

Fig. 7. Illustration of calculated DOC inlet and outlet temperature, and energy source/sink terms as functions of time.

during the cold-start. The CO mole concentration is set to 0.6% at the inlet. The DOC gas inlet temperature is assumed to increase linearly from 300 K at 1.5 K s^{-1}, and to remain constant at 600 K after 200 s.

The DOC efficiency is assumed to follow the curves shown in Fig. 3 for fresh and aged DOCs. The total mass of DOC is set to 4.0 kg. The specific heat is 1.0 kJ kg^{-1} K^{-1} and the total thermal inertia (mass multiplies specific heat) is 4000 J K^{-1}. In the calculation, the pipe outer diameter is set to 88.9 mm (3.5 in.); the pipe wall thickness set to 2.3 mm; the total length set to 0.9144 m (55 in.). Stainless steel properties are used for the pipe: density of 7500 kg m^{-3}, specific heat of 500 J kg^{-1} K^{-1}, and thermal inertia of 3000 J K^{-1}. The SCR is estimated to have a mass of 6.0 kg, specific heat of 1.0 kJ kg^{-1} K^{-1} and thermal inertia of 6000 J K^{-1}.

Fig. 6 summarizes the results of the simplified test case. At about 250 s, the DOC outlet temperature exceeds the engine-out temperature. The higher temperature in DOC is due to the exothermic reaction of CO oxidation. At steady-state, the reaction heat release from CO oxidation contributes to temperature increase by 60 K in DOC. Due to heat transfer from the pipe, the DOC outlet is seen to have a higher steady-state temperature than the SCR inlet temperature, cf., Fig. 6. When SCR outlet temperature exceeds 473 K, light-off starts at 230 s and full light-off is reached at 300 s.

The DOC light-off is critical to diesel exhaust aftertreatment system, which oxidizes CO and HC to CO_2 and H_2O, and NO to NO_2. The exothermic reaction of CO and HC oxidation is also an energy source that heats the exhaust gas downstream of the pipe and reactors (SCR and DPF). Fig. 7 summarizes the model calculation of the reaction heat release rate, the convective heat transfer rate from exhaust gas to DOC, the temperature at DOC inlet and outlet. Due to convective heat transfer, the DOC inlet and outlet temperatures increase over the time period 0–150 s. At around 150 s, CO reaction sets in. The DOC outlet temperature continues to increase and it exceeds the inlet temperature at around 260 s. The convective heat transfer direction reverses; the heat transfer rate becomes negative. The DOC warm-up process shown in Fig. 7 suggests that an effective means to reduce the DOC warm-up time must be achieved in order to meet the T2B5 emission standard.

4. Methods to shorten cold-start time

Two methods are examined. One reduces thermal inertia of the system (passive solution), and the other provides an additional heat source (active solution). These methods are discussed in the following.

The thermal inertia of the system can be reduced by using metallic DOC and/or moving SCR upstream. Typically, metallic DOC can have 15–20% less thermal inertia compared to ceramic DOC. In this work, we demonstrate that reduction of thermal inertia by using metallic DOC is not sufficient to reach the NOx reduction target. A 50% reduction of thermal inertia is examined. Moving SCR upstream also reduces the thermal inertia of the pipe. The heat loss to the surroundings is also reduced due to the reduced pipe length. Seven cases that reduce thermal inertia of the DOC and pipes are examined. Case #1 is the standard architecture case (the baseline case). Cases #2 to #7 are cases with reduced total thermal inertia from reduction of DOC and/or pipe thermal inertia. Time for the SCR inlet and outlet temperatures to reach the light-off temperature, i.e., 473 K, is summarized in Table 1. Four cases are plotted in Fig. 8; showing the SCR inlet temperatures of the baseline case (Case #1 in Table 1), the metallic DOC (Case #5; 50% DOC thermal inertia reduction), the SCR upstream (Case #2; 33% reduction of pipe length), and

Table 1
Test cases of thermal inertia reduction to reduce SCR light-off time; 7 total thermal inertia cases were considered, including the standard architecture case (Case #1) and 6 reduced thermal inertia cases from reduction of DOC and/or pipe thermal inertia (Cases #2 to #7).

	Case number						
	1	2	3	4	5	6	7
DOC thermal inertia (J K^{-1})	4000	4000	3000	3000	2000	2000	2000
Pipe thermal inertia (J K^{-1})	3000	2000	3000	2000	3000	2000	1500
Total thermal inertia (J K^{-1})	7000	6000	6000	5000	5000	4000	3500
Time forSCRinlet@473 K (s)	232	214	215	197	196	179	170
Time forSCRoutlet@473 K (s)	337	313	316	293	295	272	261

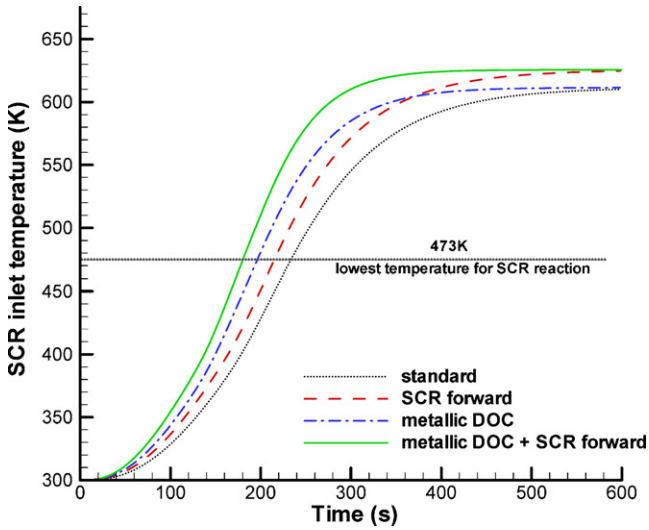

Fig. 8. Predicted SCR inlet temperature of SCR forward (Case #2), metallic DOC (Case #5), combined metallic DOC and SCR forward (Case #6), and standard (baseline; Case #1) aftertreatment architecture.

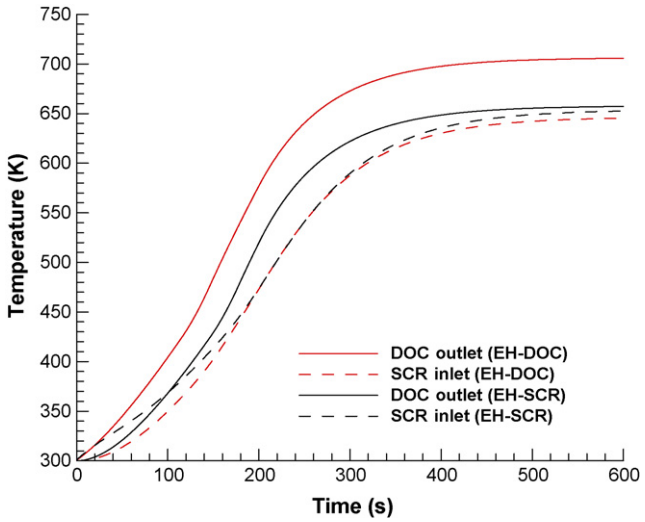

Fig. 9. Temperature as function of time at DOC and SCR inlet and outlet with applied electrical heating of 2.6 kW.

combined metallic DOC and SCR upstream (Case #6; 43% reduction of total mass).

The moving SCR upstream reduces the heat loss to the surroundings, which in term results in a higher temperature at SCR inlet. A shorter light-off time than the baseline case is achieved. The metallic DOC reduces thermal inertia from 7000 to 5000 J K^{-1}, and SCR upstream reduces it to 6000 J K^{-1}. The reduced thermal inertia increases the rate of temperature rise. The heat release from early light-off of CO oxidation accelerates the warm-up process. The net effect is that metallic DOC yields a 29% reduction of the light-off time and SCR upstream reduces 14% of the light-off time. To further reduce the light-off time, combination of metallic DOC and SCR upstream is implemented in Case #7, which results in the shortest SCR light-off time of all the conditions given in Table 1. The light-off time at SCR inlet is reduced from 232 s of the baseline case to 170 s, and that at SCR outlet is reduced from 337 to 261 s. The physical constraints of the reactor size and packaging are such that further reducing the light-off time cannot be achieved from thermal inertia and SCR upstream considerations.

To further decrease the light-off time beyond that can be achieved by passive solution, an additional energy source term with constant heating is added to the source term of Eq. (1). Both electrical heating and fuel injection into the DOC are considered. The results with electrically heated DOC (EH-DOC) and electrically heated SCR (EH-SCR) are summarized in Tables 2 and 3, respectively. The prototype aftertreatment architecture shown in Fig. 1 and Case #6 architect that uses metallic DOC and moves SCR upstream (i.e., Case #6 in Table 1) are examined.

The results summarized in Tables 2 and 3 show that 520 kJ (2.6 kW × 200 s or 0.14 kW h) is required to reduce SCR light-off time to 200 s (compared to 232 s of no external heating) for both the EH-DOC and EH-SCR configurations. The calculation also shows that EH-SCR has a shorter light-off time than EH-DOC with the same heating rate. For the EH-DOC, the electrical energy is used to heat DOC directly and indirectly to SCR and the pipe connecting DOC and SCR. As for EH-SCR, the energy is only used to heat SCR and it results in a shorter light-off time. The calculation also shows that the higher rate of electrical heating the greater the differences are between the EH-DOC and EH-SCR results.

The aftertreatment architecture optimization has resulted in energy saving. By architecture optimization, the SCR light-off can start as early as 170 s. In order to achieve the same target with the prototype architecture system, 825 kJ (4.85 kW, 170 s) and 918 kJ (5.4 kW, 170 s) is required for EH-SCR and EH-DOC, respectively. The combination of architecture optimization (e.g., Case #6 or #7 of Table 1) and external energy supply can reduce SCR light-off time more effectively. Architecture optimization reduces the light-off time by about 60 s. The 2.6 kW heating reduces the light-off time by about 30 s. Combination of the optimized aftertreatment architecture and 2.6 kW heating reduces the light-off time by about 90 s. Compared to the pure electrical heating, the energy consumption for Case #6 configuration is reduced by 25% (or around 78 J), along with a shorter heating time, i.e., 147–154 s vs. 200 s. The CO oxidation from the earlier DOC light-off provides an extra 30 s for CO oxidation that accounts for about 93 kJ heating when 100% oxidation of the 0.6% mole CO in the exhaust gas is achieved.

Table 2
Results for DOC with electrical heating (EH-DOC); prototype architect shown in Fig. 1 was used unless specified otherwise.

Energy input (kW)	0	1	2.6	2.6[a]	4	5.4	13.95
Time forSCRinlet@473 K (s)	232	219	200	147[a]	185	170	111
Time forSCRoutlet@473 K (s)	337	320	297	238[a]	280	265	200

[a] Case #6 aftertreatment architecture given in Table 1 (metallic DOC and SCR forward).

Table 3
Results for SCR with electrical heating (EH-SCR); prototype architect shown in Fig. 1 was used unless specified otherwise.

Energy input (kW)	0	1	2.6	2.6[a]	4	4.85	9.75
Time forSCRinlet@473 K (s)	232	220	200	154[a]	182	170	96
Time forSCRoutlet@473 K (s)	337	319	293	240[a]	272	261	200

[a] Case #6 aftertreatment architecture given in Table 1 (metallic DOC and SCR forward).

Table 4
Results for DOC with electrical heating (EH-DOC)—new scenario.

Energy input (kW)	0	1	2	3	4	5	6.9
Time forSCRinlet@473 K (s)	184	172	160	148	138	127	111
Time forSCRoutlet@473 K (s)	276	262	249	238	227	217	200

Table 5
Results for SCR with electrical heating (EH-SCR)—new scenario.

Energy input (kW)	0	1	2	3	4	5	7.5
Time forSCRinlet@473 K (s)	184	176	167	159	150	141	111
Time forSCRoutlet@473 K (s)	276	264	253	242	232	223	200

Fig. 9 summarizes the temperature evolution at inlets and outlets of EH-DOC and EH-SCR. Initially, EH-SCR results in higher SCR inlet temperatures as it reaches light-off sooner than EH-DOC. The EH-DOC has an earlier light-off at DOC. The reaction heat release from CO oxidation helps to reduce the temperature difference at SCR inlets. After DOC outlet temperature also reaches the light-off condition, the same amount of reaction heat is released from CO oxidation for both systems; similar temperatures are observed for time greater than 200 s. Considering the same amount of energy provided for the two cases, EH-SCR has higher energy input per unit thermal inertia as heating is applied to SCR only, while heating at EH-DOC is applied to DOC, as well as to the pipe and SCR. As the result, EH-SCR again shows higher SCR inlet temperatures than EH-DOC.

Caution should be exercised on the above observation that EH-SCR performs better than EH-DOC in regard to the reduction of SCR light-off time. The reverse will be the case when the aftertreatment is consisted of a DOC with a lower thermal inertia (e.g., 2000 J K^{-1}) and a higher CO concentration (1.2%) is present in the exhaust gas. Tables 4 and 5 summarize the results of this new scenario. As can be seen from the tables, the EH-DOC outperforms EH-SCR for the power settings in the range of 1–5 kW; EH-DOC requires a lower wattage of 6.9 kW to reach the light-off temperature at 111 s; whereas 7.5 kW is required by EH-SCR. Because of the relatively small thermal inertia of DOC given in Tables 4 and 5, DOC can light-off rather quickly. Together with the relatively high CO concentration, more reaction heat is released to heat-up the downstream SCR. The net consequence is that EH-DOC outperforms EH-SCR for this scenario.

5. Summary and conclusion

The energy balance method is a viable tool for system-level analysis of the aftertreatment performance. The model is validated by temperature data of a prototype aftertreatment of a 4.5 l diesel engine. The simulation shows that the SCR light-off time can be reduced by system thermal inertia reduction. For example, with overall 43% thermal inertia reduction, the SCR light-off time reduces from 232 to 170 s at SCR inlet and from 337 to 261 s at SCR outlet. Electrical heating to shorten SCR light-off time is also examined. To reach the target 200 s of light-off at SCR inlet, 520 kJ is required for EH-SCR and EH-DOC; 1950 and 2790 kJ are required for EH-SCR and EH-DOC to reach the target time at SCR outlet.

Optimization of the aftertreatment architecture (i.e., that reduces thermal inertia) can reduce or eliminate the level of electrical heating to achieve the same light-off time. For example, the optimized architecture, Case #6, can achieve an SCR light-off time of 170 s at inlet, which cannot be achieved with the baseline architecture without applying external heating to SCR or DOC. The system architecture optimization, however, is subject to vehicle under-hood packaging restrictions. To meet more stringent emission standards in the future, combination of architecture optimization and electrical heating will be required.

Acknowledgments

The authors thank Charles Solbrig at GM powertrain for providing the test cell data and the architecture information about the diesel engine aftertreatment system. Also the authors thank David, B. Brown at GM powertrain for the explanation about water condensation and ammonium nitrate formation inside SCR.

References

[1] C.R. Ferguson, A.T. Kirkpatrick, Internal Combustion Engines, 2nd ed., John Wiley & Sons, New York, NY, 2001.
[2] A. Fritz, V. Pitchon, The current state of research on automotive lean NOx catalysis, Appl. Catal. B 13 (1997) 1–25.
[3] Y.S. Cheng, H.C. Yeh, J.L. Mauderly, B.V. Mokler, Characterization of diesel exhaust in a chromic inhalation study, AIHA J. 45 (1984) 547–555.
[4] M. Shelef, Selective catalytic reduction of NOx with N-free reductants, Chem. Rev. 95 (1995) 209–225.
[5] S.H. Oh, E.J. Bissett, Mathematical modeling of electrically heated monolith converters: analysis of design aspects and heating strategy, Ind. Eng. Chem. Res. 33 (1994) 3086–3093.
[6] R.M. Heck, R.J. Farrauto, Automobile exhaust catalysts, Appl. Catal. A 221 (2001) 443–457.
[7] G. Groppi, E. Tronconi, P. Forzatti, Mathematical models of catalytic combustors, Catal. Rev. Sci. Eng. 41 (1999) 227–254.
[8] C. Depcik, D. Assanis, One-dimensional automotive catalyst modeling, Prog. Energy Combust. Sci. 31 (2005) 308–369.
[9] Y. He, Development of an integrated diesel exhaust aftertreatment simulation tool with applications in aftertreatment system architecture design, SAE paper, 2007-01-1138.
[10] P. Koci, M. Kubicek, M. Marek, Periodic forcing of three-way catalyst with diffusion in the washcoat, Catal. Today 98 (2004) 345–355.
[11] R.B. Bird, W.E. Stewart, E.N. Lightfoot, Transport Phenomena, John Wiley & Sons, New York, NY, 1960.
[12] C.S. Sampara, E.J. Bissett, M. Chmielewski, D. Assanis, Global kinetics for platinum diesel oxidation catalysts, Ind. Eng. Chem. Res. 46 (2007) 7993–8003.
[13] Y. Miao, GMT901 aftertreatment system cold-start analysis, General Motors Co. Internal Report, Warren MI, 2009.
[14] K. Narayanaswamy, Y. He, Modeling of copper-zeolite and iron-zeolite selective catalytic reduction (SCR) catalysts at steady-state and transient conditions, SAE paper, 2008-01-0615.
[15] Y. He, Development of an integrated diesel exhaust aftertreatment simulation tool with application in aftertreatment system architecture design, SAE paper 2007-1-1138.